GLP1R agonists activate human POMC neurons

Simone Mazzaferro[1,2], Hsiao-Jou Cortina Chen[1,2], Oliver Cahn[1,2], Andrian Yang[1-3], Dmytro Shepilov[1,4], Jiahui Chen[1,2], Contanza Alcaino[1], Viviana Macarelli[1,2], Iman Mali[1,5], Fiona Gribble[1], Frank Reimann[1], John Marioni[3,6-8], Florian T. Merkle*[1,2]

[1]Institute of Metabolic Science, University of Cambridge, Cambridge CB2 0QQ, UK
[2]Cambridge Stem Cell Institute, University of Cambridge, Cambridge CB2 0AW, UK
[3]European Molecular Biology Laboratory, European Bioinformatics Institute, Wellcome Genome Campus, Hinxton, CB10 1SD, UK
[4]Department of Cytology, Bogomoletz Institute of Physiology, National Academy of Sciences of Ukraine, Kyiv, 01024, Ukraine
[5]Victor Phillip Dahdaleh Heart and Lung Research Institute, Royal Papworth Hospital NHS Foundation Trust, University of Cambridge, Cambridge, CB2 0BB, UK.
[6]Wellcome Sanger Institute, Wellcome Genome Campus, Hinxton, CB10 1SD, UK
[7]Cancer Research UK Cambridge Institute, University of Cambridge, Cambridge, CB2 0RE, UK
[8]Genentech, South San Francisco, CA, 94080, USA.

*address for correspondence: fm436@cam.ac.uk

Key words: GLP-1, GLP1R, POMC, Semaglutide, Tirzepatide, obesity, iPSC, hypothalamus

Abstract

Drugs like Semaglutide (a.k.a. Ozempic/Wegovy) that activate the glucagon-like peptide-1 receptor (GLP1R) are a promising therapy for obesity and type 2 diabetes (T2D). Animal studies suggest that appetite-suppressing proopiomelanocortin (POMC) neurons in the arcuate nucleus of the hypothalamus are a likely target of these drugs, but the mechanisms by which they reduce food intake in humans are still unclear. We therefore generated POMC neurons from human pluripotent stem cells (hPSCs) to study their acute responses to GLP1R agonists by calcium imaging and electrophysiology. We found that hPSC-derived POMC neurons expressed *GLP1R* and many of them robustly responded to GLP1R agonists by membrane depolarization, increased action potential firing rate, and extracellular calcium influx that persisted long after agonist withdrawal and was likely mediated by L-type calcium channels. Prolonged administration of Semaglutide upregulated transcriptional pathways associated with cell survival in POMC neurons, and downregulated pathways associated with oxidative stress and neurodegeneration. These findings suggest that POMC neurons contribute to the long-term appetite-suppressive effects of GLP1R agonists in humans.

Introduction

Obesity affects over a billion people worldwide and significantly increases the risk of chronic diseases such as type 2 diabetes and cardiovascular disease (NCD Risk Factor Collaboration (NCD-RisC) 2024). It has a very strong genetic basis, and genetic variants associated with obesity predominantly act in the brain (Locke et al. 2015). Studies of individuals with severe, early-onset obesity revealed mutations in brain circuits that are essential for appetite regulation, such as the leptin-melanocortin system (van der Klaauw et al. 2019; S. Farooqi and O'Rahilly 2006; Loos and Yeo 2022). Specifically, populations of

pro-opiomelanocortin (POMC) neurons in the arcuate nucleus of the hypothalamus increase their firing rate in response to the adipocyte-derived hormone leptin (Cowley et al. 2001; Qiu et al. 2018) and the predominantly gut-derived hormone glucagon-like peptide-1 (GLP-1) (Gabery et al. 2020; Secher et al. 2014; Dong et al. 2021; Péterfi et al. 2021). Activated POMC neurons then release more of the POMC-derived peptides α-melanocyte stimulating hormone (α-MSH) and β-MSH (Kirwan et al. 2018; Lee et al. 2006) that stimulate the melanocortin 4 receptor (MC4R) on neurons that suppress food intake and increase energy expenditure (Fenselau et al. 2017; Baldini and Phelan 2019; Cone 2005). Although other appetite-regulatory cell populations respond to GLP-1, including cells of area postrema (AP) (Kawatani, Yamada, and Kawatani 2018) and nucleus tractus solitarius (NTS) of the hindbrain (Hayes et al. 2011), the loss of either *POMC* or *MC4R* is sufficient to increase appetite and body weight in both humans (I. S. Farooqi et al. 2003; Yeo et al. 2003; Krude et al. 1998) and animals (Dittmann et al. 2024; Yaswen et al. 1999; Huszar et al. 1997), demonstrating that POMC neurons are essential for normal long-term body weight regulation.

The ability of GLP-1 to suppress appetite has recently been harnessed by modified peptide agonists of the GLP-1 receptor (GLP1R) that are revolutionizing the treatment of T2D and obesity (Meier 2012; Bessesen and Van Gaal 2018; Tan et al. 2022). GLP1R agonists delay gastric emptying and reduce food intake in humans to reduce body weight and improve metabolic health for long periods of time (Halawi et al. 2017). The efficacy of GLP1R agonist monotherapies such as Semaglutide (a.k.a. Ozempic, Wegovy) can be further improved by combining it with agonism of the gastric inhibitory polypeptide receptor (GIPR) and/or the glucagon receptor (GCGR) (Knerr et al. 2022; Coskun et al. 2022; Zhao et al. 2022), but some users experience side effects with these drugs, and their efficacy still falls short of what is seen with bariatric surgery.

To rationally design more effective treatments for obesity, it is important to understand the mechanisms by which existing treatments work in humans. GLP1R signaling has been well-studied in pancreatic β-cells (Shilleh et al. 2024), where its coupling to $G_{\alpha s}$ stimulates adenylate cyclase to elevate the intracellular concentration of cyclic adenosine monophosphate, or $[cAMP]_i$. This in turn activates protein kinase A (PKA) which increases the influx of extracellular Ca^{2+} through L-type voltage-gated calcium channels to promote insulin secretion (Gomez, Pritchard, and Herbert 2002). GLP1R can also couple to β-arrestin upon ligand binding, which promotes its rapid internalization (Sonoda et al. 2008) and continued signaling from the endosome (Irannejad et al. 2013). In the nervous system, signaling pathways downstream of GLP1R are less well understood but likely also involve $G_{\alpha s}$ coupling, since PKA becomes activated in NTS neurons (Hayes et al. 2011). Due to the inaccessibility of human neurons, endogenous GLP1R signaling pathways are unknown, and extrapolating insights from rodent studies is hampered by species-specific differences in appetite-regulatory cell types (Steuernagel et al. 2022; Tadross et al. 2023; Kirwan et al. 2018).

To address these limitations, we derived hypothalamic POMC neurons from human pluripotent stem cells (hPSCs), including a *POMC-GFP* knock-in reporter cell line that enabled their prospective identification in live cultures. We found that many human POMC neurons expressed *GLP1R* mRNA and were durably activated by GLP-1 and other GLP1R agonists including Exendin-4 derivatives, Semaglutide, and the dual GLP1R/GIPR agonist Tirzepatide (a.k.a. Mounjaro). Electrophysiological recordings and pharmacological studies suggested that POMC neurons were depolarized by GLP1R agonists for at least 20 minutes and fired substantially more action potentials via mechanisms that required functional L-type

calcium channels. Prolonged stimulation with Semaglutide also induced significant transcriptional changes in human POMC neurons related to cell survival and neurodegenerative pathways. Together, these studies suggest that the activation of POMC neurons likely contributes to the appetite-suppressing effects of GLP1R agonist drugs in humans.

Results

Human hypothalamic neurons express *GLP1R*

To facilitate the study of human POMC neurons, we differentiated them from a *POMC-GFP* knock-in cell line in which GFP is co-translationally expressed with the endogenous POMC gene (Chen, Yang, et al. 2023). This cell line allows live GFP+ POMC neurons to be prospectively identified and studied by fluorescent microscopy (Fig. 1A,B). To determine if these hPSC-derived neurons could be useful for the study of human GLP1R biology, we first analyzed single-cell transcriptomic data from five genetically distinct hPSC lines that were differentiated to hypothalamic cells (Chen, Yang, et al. 2023) (Fig. 1C). Whereas only a median of 1.1% of cells expressed *GLP1R* (UMI ≥ 1) across all clusters, *GLP1R* transcript was detectable at appreciable levels (>10% of cells) in cell clusters annotated as POMC neurons (2578/22892 cells, 11.3%), or OTP+ SST+ neurons (1424/12641 cells, 11.3%) (Fig. D,E). These findings suggest that POMC neurons are enriched in GLP1R expression. To further validate these results, we tested for *GLP1R* expression in the *POMC-GFP* cell line and found that 594/7634 (7.8%) of the *GFP*-expressing (UMI ≥ 1) cells in the POMC cell cluster also expressed *GLP1R*.

The observed *GLP1R*+ POMC neuron percentages are lower than the 37-100% of rodent POMC neurons reported to functionally respond to GLP1R agonists (Rønnekleiv et al. 2014; He et al. 2019; Péterfi et al. 2021; Secher et al. 2014). We reasoned that this discrepancy might be due to either the immaturity of hPSC-derived cells relative to their counterparts in the adult brain, or the inefficiency of transcript capture in single-cell data. Specifically, single-cell sequencing methods systematically underestimate the fraction of cells positive for genes expressed at low to moderate levels (Brennecke et al. 2013), such as G-protein coupled receptors like *GLP1R*. We therefore tested for *Glp1r* expression (UMI ≥ 1) in an integrated single-cell and single-nucleus RNAseq atlas of 384,925 mouse hypothalamic cells (Steuernagel et al. 2022). We found that mouse hypothalamic cell clusters annotated as Pomc neurons (C66-19) (Fig. 1F, arrow) or Sst neurons (C66-47) expressed *Glp1r* in 380/4655 (8.2%) and 479/5414 (8.8%) of cells, respectively, while the median percentage of *Glp1r*-expressing cells in other clusters was 1.1%. (Fig. 1G,H). These findings are similar to those seen in hPSC-derived hypothalamic cultures (Fig. 1E), suggesting that the modest fraction of *GLP1R*+ human and mouse POMC neurons we observed is likely attributable to inefficient mRNA capture in single-cell data rather than cellular immaturity. Together, these results demonstrate that hPSC-derived POMC neurons express *GLP1R*, and suggest that broad cell type-specific expression patterns of this gene are similar between the mouse and human hypothalamus.

GLP-1 activates human POMC neurons

The expression of *GLP1R* on human POMC neurons suggested that they might functionally respond to GLP-1 peptide and other GLP1R agonists. Since these agonists increase the electrical activity of rodent POMC neurons (Péterfi et al. 2021; Secher et al. 2014; Dong et al. 2021; Rønnekleiv et al. 2014; He et al. 2019; Singh et al. 2022), which

raises their intracellular calcium concentration or $[Ca^{2+}]_i$, we used calcium imaging to test for GLP1R agonist-induced calcium responses in human hypothalamic neurons derived from a *POMC-GFP* knock-in hPSC line. We loaded cultures of hypothalamic neurons derived from this cell line with a red calcium-sensitive dye (Fig. 2A), and imaged them on an upright microscope in a buffered physiological recording medium (HBSS) fed by a gravity perfusion system. All media and solutions contained synaptic blockers to isolate cell-autonomous responses from network activity. We selected cells for analysis if they exhibited stable baseline fluorescence and showed a clear increase in fluorescence ($\Delta F/F_0$) in response to a depolarizing stimulus of 50 mM KCl (Fig. 2B-D), which we observed for the vast majority or recorded cells. These findings suggested that hPSC-derived hypothalamic neurons were electrophysiologically capable of responding to depolarising stimuli.

Next, we diluted GLP-1 peptide to a final concentration of 200 nM in recording media with synaptic blockers, since similar concentrations of GLP1R agonists (100 nM - 1 μM) were previously used used in studies with rodent slice cultures (He et al. 2019; Péterfi et al. 2021; Secher et al. 2014; Gabery et al. 2020; Dong et al. 2021). After 10 minutes of recording to identify cells with stable baseline fluorescence, we added GLP-1 to cultures for two minutes followed by a wash-out period of 10-20 minutes and a terminal application of 50 mM KCl. Upon identifying hypothalamic neurons with stable baseline fluorescence and robust responses to KCl, we found that some such cells did not respond to GLP-1 (Fig. 2B), whereas others showed decreased (Fig. 2C) or increased (Fig. 2D) fluorescence intensity that persisted for tens of minutes, suggesting prolonged $[Ca^{2+}]_i$ changes indicative of inhibition or activation, respectively.

To categorize non-responsive, inhibited, and activated cells in an unbiased manner, we tested for significant differences between mean fluorescence intensities at 18 time points in a three-minute pre-stimulus window just before GLP-1 addition, and a three-minute post-stimulus window after GLP-1 wash-out, when responses in activated or inhibited cells had plateaued (Fig. 2E). We conservatively defined responsive cells as those having significant ($P < 0.01$) changes in $\Delta F/F_0$, and either activated or inhibited depending on the direction of the response, whereas we defined cells whose response fell below this significance threshold non-responsive (Fig. 2F). Using these criteria, we found that the majority of GFP+ POMC neurons (6/10, 60%) were activated by 200 nM GLP-1. In contrast, few (25/154, 16%) GFP- neurons were activated and some (15/154, 10%) appeared to be inhibited (Fig. 2F). We then quantified the response magnitudes by calculating the post-stimulus area under the curve (AUC) normalized to the pre-stimulus AUC (Fig. 2G) calculated using the same time windows used for significance testing for both GFP- and POMC neurons (Fig. 2H). Since we observed both activated and inhibited populations among GFP- cells (Fig. 2F,H) but only activated POMC neurons, these results suggested cell type-specific responses. We therefore hypothesized that probing GLP1R signaling using biased agonists might shed light on the observed divergent responses.

<u>'Biased' GLP1R ligands alter the fraction of cells displaying inhibitory responses</u>

Based on studies in the rodent CNS, GLP1R is thought to predominantly couple to $G_{\alpha s}$ and/or β-arrestin (Jorgensen et al. 2007; Wootten et al. 2016; Sonoda et al. 2008). We therefore treated hPSC-derived neurons with 'biased' GLP1R agonists thought to preferentially engage these distinct pathways. Specifically, F^1-Exendin-4 (Ex-F1) is thought to preferentially engage $G_{\alpha s}$ to promote GPCR-mediated cAMP production and $[Ca^{2+}]_i$ increase, whereas D^3-Exendin-4 (Ex-D3) is more readily internalized in a β-arrestin-dependent manner (Jones et al. 2018). We therefore exposed cells to either 200

nM Ex-F1 or 200 nM Ex-D3. We found that responsive POMC neurons were exclusively activated (14/14, 100%) by Ex-F1, whereas 28/40 (70%) of responding GFP- neurons were activated and 12/40 (30%) were inhibited (Fig. 3A-C). In contrast, only 5/7 (71%) of responding POMC neurons and 20/36 (55.5%) of responding GFP- neurons were activated by Ex-D3, respectively (Fig. 3D-F). The fraction of activated cells was significantly higher ($P<0.05$) in response to Ex-F1 (42/54, 78%) than to Ex-D3 (25/43, 58%), suggesting that GLP1R ligand structure can trigger distinct neuronal calcium responses.

Next, we hypothesized that cells should remain responsive to GLP1R ligands that do not effectively induce receptor internalization (e.g. Ex-F1), whereas cells should lose responsiveness to ligands that promote internalization (e.g. Ex-D3). We therefore exposed hypothalamic cultures to either 200 nM Ex-F1 or Ex-D3 for two minutes, washed ligands off for 10 minutes, and again exposed them to the same ligands for another two minutes and recorded cellular responses. We then compared $\Delta F/F_0$ in three minute windows taken before and after the second ligand administration and found that 9/14 (64%) POMC neurons that had initially responded to Ex-F1 again responded to a second administration (Fig. 3A), whereas none of the seven (0%) POMC neurons exposed to Ex-D3 showed such a second response (Fig. 3D). These results suggest that either receptor internalization removes the pool of GLP1R necessary to generate responses detectable in our experimental system, or that these two ligands are engaging distinct intracellular signaling pathways.

Effect of GLP1R agonist drugs

Intrigued by the responses of human POMC neurons to GLP-1 and Exendin-4 analogues, we wondered how they would respond to GLP-1 derivative drugs that are clinically used to treat T2D and obesity. We therefore treated hPSC-derived hypothalamic cultures with 200 nM Semaglutide (Lau et al. 2015; Wilding et al. 2021) or the dual GLP1R/GIPR agonist Tirzepatide (Coskun et al. 2018; Jastreboff et al. 2022) and compared their responses to those observed with 200 nM GLP-1 (Fig. 4A-C). Among the 29 analyzed POMC neurons and 148 GFP- cells treated with Semaglutide (Fig. 4D-F), significantly more ($P<0.05$) POMC neurons (20/29, 69%) than GFP- cells (56/148, 39%) showed a detectable response. Among responding cells, Semaglutide predominantly activated both POMC neurons (19/20 cells, 95%), and GFP- neurons (46/56 cells, 82%), in contrast to the responses seen in GFP- neurons to GLP-1 (25/40, 63%) or ex-D3 (25/43, 58%) (Fig. 3). Similarly, in response to Tirzepatide, significantly ($P<0.05$) more POMC neurons (9/9, 100%) than GFP- cells (40/96, 42%) responded, and among responding cells the vast majority of both POMC neurons (8/9, 89%) and GFP- cells (37/40, 93%) were activated (Fig. 4G-I). Overall, we found that the majority of analyzed POMC neurons showed significant responses to 200 nM GLP-1, Semaglutide, or Tirzepatide (Fig. 4B,E,H), and these responses nearly always increased $[Ca^{2+}]_i$ and persisted for the entire length of the recording until KCl was added (10-20 minutes) (Fig. 4A,D,G).

Semaglutide depolarises human POMC neurons

Persistent increases in $[Ca^{2+}]_i$ could be caused by the Ca^{2+} release from internal stores such as the endoplasmic reticulum, or from neuronal depolarization and the entry of extracellular Ca^{2+} through calcium and non-selective cation channels. Electrophysiological recordings from hypothalamic mouse brain slices demonstrated that GLP-1 or Liraglutide stimulation depolarized POMC neurons in a manner that was dependent on the presence of GLP1R and that persisted for at least tens of minutes after agonist removal (Secher et al.

2014; Dong et al. 2021). We therefore hypothesized that the prolonged nature of the calcium signal we observed was due to the elevated action potential firing rate of POMC neurons.

To test this hypothesis, we performed electrophysiology of hPSC-derived GFP+ POMC neurons using a perforated patch preparation under a gravity-driven perfusion system in a buffer of HBSS. All cells in which we injected a modest amount of current (5 pA, 1 second) were able to fire trains of action potentials (3/3, 100%) and most cells (5/7, 71%) showed spontaneous action potentials in the absence of current injection, suggesting that hPSC-derived POMC neurons were healthy and capable of stimulus-evoked electrical activity. Next, we selected cells for analysis that had a membrane potential (Vm) under baseline conditions of -80 ± 15 mV, and that gave stable recordings for at least 10 minutes before and 20 minutes after administration of 200 nM Semaglutide for 6 minutes in HBSS, followed by a wash-out period in HBSS. We found that while the baseline activity of POMC neurons was low to moderate (Fig. 5A, see also E), their membrane potential and rate of action potential firing increased upon administration of Semaglutide (Fig. 5B), and persisted at elevated levels for at least 20 minutes after washout (Fig. 5C). We observe similar results from all cells tested (3/3, 100%) including both a significant ($P<0.05$) depolarization of their membrane potential by an average of 22.4 ± 3.8 mV (Fig. 5D), and a consistently increased rate of action potentials fired per minute (Fig. 5E), though firing activity varied from cell to cell. Together, these results suggest that the persistent elevation of $[Ca^{2+}]_i$ we observed in POMC neurons upon Semaglutide is likely caused by their increased electrical activity and the accompanying influx of extracellular calcium.

<u>Neuronal responses to Semaglutide require L-type calcium channels</u>

The persistent electrical activation of human POMC neurons in response to Semaglutide might increase $[Ca^{2+}]_i$ via voltage-gated calcium channels as described in pancreatic β-cells, where L-type calcium channels are engaged upon GLP1R agonist binding (Gomez, Pritchard, and Herbert 2002). We therefore examined scRNAseq data of hPSC-derived POMC and non-POMC neurons, and found that most calcium channels we tested for were expressed at some level, and POMC neurons were significantly enriched in *CACNA1D* relative to non-POMC neurons (Fig. 6A). To identify which calcium channels might contribute to the prolonged increase in $[Ca^{2+}]_i$ we observed, we treated cultures with 200 nM Semaglutide for two minutes to identify activated cells, waited for responses to plateau, and then added a cocktail of voltage-gated calcium channel (VGCC) blockers. These VGCC blockers included Benidipine (blocks L-type, N-type, and T-type channels), TTA-P2 (blocks T-type channels) and ω-Agatoxin (blocks P/Q-type channels) (Zamponi et al. 2015) (Fig. 6B). We found that upon adding these channel blockers, calcium indicator dye fluorescence dropped precipitously, sometimes below pre-stimulation baseline levels (Fig. 6C). These findings suggest that Semaglutide-induced increases in $[Ca^{2+}]_i$ require VGCCs, rather than being due to Ca^{2+} release from internal stores.

To identify which channel blockers drove this effect, we repeated these studies with one candidate VGCC blocker at a time. We saw no significant drop in fluorescence intensity in Semaglutide-activated cells upon administration of either ω-Agatoxin (8 cells, Fig. 6D,E) or TTA-P2 (21 cells, Fig. 6F,G), but observed a significant ($P<0.01$) drop in fluorescence intensity in response to the L-type-specific blocker Benidipine (11 cells, Fig. 6H,I). To replicate these findings, we tested the effects of a second L-type calcium channel blocker, Nifedipine, on Semaglutide-activated cells and again observed a significant ($P<0.0001$) drop in fluorescence intensity (34 cells, Fig. 6J,K). Together, these findings suggest that L-type

voltage-gated calcium channels are required for the sustained increase in $[Ca^{2+}]_i$ observed in human POMC neurons.

Long-term treatment with Semaglutide alters gene expression in POMC neurons

The sustained activation we observed in human POMC neurons resembled that seen in mouse POMC neurons in brain slices in response to GLP1R agonists (He et al. 2019; Péterfi et al. 2021; Secher et al. 2014; Gabery et al. 2020; Dong et al. 2021) that, on the time frame of hours to days, suppresses appetite due to increased MSH release (Baldini and Phelan 2019). We therefore wondered what transcriptional changes might accompany the sustained activation of human POMC neurons, and treated replicate cultures of hypothalamic cells differentiated from *POMC-GFP* reporter hPSCs with vehicle or Semaglutide for 20 hours. We then dissociated six replicate cultures per treatment group, purified POMC neurons by FACS, and analyzed their transcriptomes by bulk RNA sequencing. After adjusting for multiple comparisons, we found that Semaglutide induced significant (FDR<0.05) changes in gene expression, including 393 significantly down-regulated and 257 significantly up-regulated genes (Fig. 7A), of which 23 and 107 genes showed a $|\log_2(\text{fold-change})|>0.5$, respectively. To gain insight into the pathways regulated by Semaglutide treatment in POMC neurons we performed gene ontology analysis of differentially expressed genes against the Kyoto encyclopedia of genes and genomes (KEGG) pathway database (Kanehisa et al. 2023). We observed a significant upregulation of pathways associated with cell survival and cancer (Fig. B), and a significant downregulation of pathways associated with oxidative stress and neurodegeneration, among others (Fig. C).

Upregulated genes included members of multiple signaling pathways including FGF (*FGF8*, *FGF17, FGFR1*, *FGFRL1*), WNT (*FZD7, WNT5A*) and Hedgehog (*GLI2, GLI3*), whereas downregulated genes included multiple members of a key mitochondrial ATP synthase (*ATP5F1E, ATP5F1B, ATP5F1A, ATP5MF, ATP5PF*), and vacuolar H+ pumps important for the acidification of intracellular organelles including synaptic vesicles, and receptor-mediated endocytosis (*ATP6V0B, ATP6V0C, ATP6V0E2, ATP6V1B2, ATP6V1G1, ATP6V1G2, ATP6AP1*). We also observed the differential expression of genes that may help sustain higher levels of neuronal activity, including increased expression of the voltage-gated L-type calcium channel *CACNA1D* and decreased expression of the inward rectifying potassium channel *KCNJ12*. Notably, *CACNA1D* is enriched in hPSC-derived POMC neurons and is a target of the L-type blockers we applied (Fig. 6C, H-K), Together, these pathways suggest that prolonged exposure to Semaglutide alters POMC neuron cell state, which may be relevant for their responses to long-term treatment with anti-obesity drugs targeting GLP1R.

Discussion

The remarkable success of GLP1R agonist drugs in humans follows a long history of research in animal models, where cell populations in the hindbrain and hypothalamus that mediate its appetite-regulatory effects have been identified (Müller et al. 2019). While histological and single-cell studies confirm that *GLP1R* is expressed in the human hypothalamus (Tadross et al. 2023), the accessibility of these cells has previously precluded their functional analysis. Here, we demonstrate that many human POMC neurons and some other hypothalamic neurons functionally respond to GLP1R agonists, but that the nature of these responses varies by both cell type and ligand. We identify a likely mediator of the persistent electrical excitability of POMC neurons, and describe the transcriptional targets of

prolonged GLP1R activation in these cells. Below, we discuss the implications of these findings, remaining questions, and the strengths and limitations of our study.

We used single-cell sequencing to reveal cell populations that expressed *GLP1R* mRNA in the hPSC-derived cultures and mouse brain (Steuernagel et al. 2022). We found that the human POMC cell cluster had one of the highest percentages of *GLP1R* expressing cells in our dataset (11.3%), resembling results from mouse Pomc clusters (8.2%). Due to the relatively low sequencing coverage characteristic of single-cell sequencing and modest expression levels of GPCRs, these values likely underestimate the true percentage of POMC neurons that express functional levels of GLP1R protein. Indeed, we observed that the majority of *POMC-GFP* hPSC-derived POMC neurons responded to GLP1R agonists by calcium imaging. We considered cells to be POMC neurons if they had clearly detectable levels of GFP fluorescence, since GFP and POMC expression are tightly correlated at the protein level (Chen, Yang, et al. 2023). However, the identity of GFP- cells that responded to GLP1R agonists is unknown, other than that they were likely neuronal given their morphology and responsiveness to KCl. We were surprised to find that a small but highly reproducible fraction of these GFP- neurons appeared to reduce $[Ca^{2+}]_i$ upon administration of GLP1R agonists, as suggested by the sustained decrease in calcium indicator dye fluorescence. These findings suggest that signaling pathways downstream of GLP1R vary in a cell type-specific manner.

Electrophysiological analysis and pharmacological blockade of candidate channels suggested that the prolonged increases (at least 20 minutes) in action potential firing rate and increased $[Ca^{2+}]_i$ observed upon brief administration of these agonists was likely mediated by the increased electrical activity of POMC neurons and the associated influx of extracellular calcium through L-type calcium channels. L-type calcium channels can be indirectly modulated by GPCRs (Dolphin 2018) via the cAMP-dependent kinase PKA, which phosphorylates C-terminal serine residues (Mitterdorfer et al. 1996) to increase the likelihood of channel opening in some contexts, and accelerate recovery period (Cachelin et al. 1983). We speculate that the L-type channel CACNA1D ($Ca_V1.3$) may play a key role in the responses we observed as it is expressed at appreciable levels in hPSC-derived POMC neurons (~28 CPM based on bulk RNAseq data) and is significantly enriched relative to non-POMC neurons (Fig. 6A). Moreover, this channel is inhibited by Binidipine and Nifedipine, and is significantly upregulated transcriptionally in response to prolonged exposure to Semaglutide.

We also found that 20-hour Semaglutide treatment was associated with the significant downregulation of pathways associated with neurodegeneration. While these findings require validation and mechanistic follow-up, it has not escaped our attention that GLP1R agonists show neuroprotective and cognitive benefits to mice (During et al. 2003; Li et al. 2009; Panagaki, Gengler, and Hölscher 2018), and humans (Wu et al. 2018; Vadini et al. 2020), and are in numerous clinical trials for Alzheimer's Disease (Michael Gejl et al. 2017; M. Gejl et al. 2016; Egefjord et al. 2012), Parkinson's Disease (Aviles-Olmos et al. 2013, 2014; Hogg et al. 2022) and other neurological conditions (Mitchell et al. 2023; Glotfelty et al. 2019). The mechanisms by which GLP1R agonists exert their neuroprotective effects remain largely obscure (Reich and Hölscher 2022; Kopp et al. 2022), and our findings suggest that they could involve direct effects on neurons.

Finally, we note that the release of MSH by POMC neurons plays a dose-dependent and central role in body weight homeostasis (Biebermann et al. 2006; Baldini and Phelan 2019). Therefore, although other brain regions also likely contribute to the weight loss effects of GLP1R agonist drugs, the increased activity of POMC neurons upon acute

administration of GLP1R agonists, together with the transcriptional changes following longer-term exposure, suggests that human POMC neurons are likely one of their mechanistic targets.

Limitations of study

Though we took care to ensure the reproducibility and relevance of our work, we acknowledge several limitations. First, much of our work was based on a single cell line (*HUES9-POMC-GFP*) analyzed at time points when cells were sufficiently mature to fire spontaneous action potentials and show clear calcium responses. Although POMC neurons from this cell line closely resemble POMC neurons derived from diverse genetic backgrounds at the transcriptional level (Chen, Yang, et al. 2023), it is possible that different results could have been obtained on different genetic backgrounds, maturation time points, or in different culture conditions. Furthermore, while we reduced the likelihood of recorded activity being driven by network activity with the use of a synaptic blocker cocktail in all experiments, we cannot formally exclude the possibility that cells communicated with each other via other mechanisms, such as gap junctions or paracrine signals.

We tested the hypothesis that L-type calcium channels are required for sustained GLP1R agonist-mediated activation of POMC neurons and found evidence supporting this hypothesis. However, other channels may also contribute. For example, in mouse hypothalamic hypocretin (HCRT) neurons, Exendin-4 induced an extracellular sodium-dependent and intracellular GDP-dependent depolarization and inward current in the absence of extracellular Ca^{2+} consistent with G-protein dependent depolarization and the involvement of a non-selective cation channel (Acuna-Goycolea and van den Pol 2004). We found that brief administration of GLP1R agonists typically resulted in prolonged POMC neuron activation over a period of up to 20 minutes. In future studies, it would be interesting to determine the full duration of this increased activity, the kinetics by which $[Ca^{2+}]_i$ returns to baseline, and compare these kinetics to any changes in intracellular cAMP concentrations to study responses more proximal to putative GLP1R-$G_{\alpha s}$ coupling.

Much attention has been paid to the heterogeneity of POMC neurons based on the genes they express, their anatomical location and connectivity, or by their functional responses to factors like leptin and GLP-1 as determined by electrophysiological recording or calcium imaging (Quarta et al. 2021). There is little agreement about the identity of these POMC sub-populations, or how identified mouse sub-populations might map onto the human counterparts. Specifically, differences seen between mouse and human datasets could be attributable to true species-specific differences, the maturation state of adult mouse versus hPSC-derived human cells, or technical factors such as sequencing depth or library quality. In order to draw robust conclusions about functionally relevant human POMC neuron heterogeneity, further functional and molecular characterization that is beyond the scope of the current study is necessary. This includes cAMP imaging and characterization of POMC neuron responses to a broad panel of candidate ligands, followed by confirmation in primary human brain tissue or in snRNAseq data. Finally, we did not consider non-hypothalamic cell populations in this study, and it would be of great interest to study other GLP1R-responsive human neuron types, such as NTS neurons.

Materials and methods

Analysis of single-cell sequencing data

Processed single-cell RNA sequencing data obtained from five distinct hPSC lines differentiated to hypothalamic neurons (Chen, Yang, et al. 2023) as well as published data from HypoMap mouse single cell hypothalamus atlas (Steuernagel et al. 2022) were analyzed for the expression of *GLP1R* and other genes of interest using expression cutoffs of ≥1 UMI.

Human pluripotent stem cell (hPSC) culture and hypothalamic differentiation

All cultures were maintained at 37°C in humidified incubators at 5% CO_2 and 20% O_2. Human pluripotent stem cell (hPSC) line HUES9-*POMC-GFP* (passage 12-18 after reporter generation) was generated (Chen, Yang, et al. 2023) and maintained as previously described (Chen, Mazzaferro, et al. 2023). Briefly, stem cells were maintained on Geltrex-coated plates in StemFlex medium and passaged upon reaching ~70% confluence with 0.5 mM EDTA in the presence of 10 µg/mL Rock Inhibitor Y-27632.

These cell lines were then differentiated into hypothalamic neurons as previously described (Chen, Mazzaferro, et al. 2023; Merkle et al. 2015; Kirwan, Jura, and Merkle 2017). Briefly, hPSCs were dissociated to a single-cell suspension and plated onto Geltrex-coated plates at a density of $1x10^5$ cells/cm^2 in StemFlex medium supplemented with 10 µg/mL Rock Inhibitor Y-27632. The following day, media was changed to N2B27 media containing small molecule BMP, TGFβ and WNT inhibitors to promote neural induction, followed by small molecule SHH agonists to promote ventralization. On day 13 of differentiation, hypothalamic progenitors were dissociated with a mixture of TrypLE Express and 200 U/mL papain, washed with media supplemented with 2 mg/mL DNAse I (1:60), and re-plated at a concentration of $2.5x10^5$ cells/cm^2 onto plates coated with 4 µg/mL iMatrix-511 (Takara Bio) in N2B27 medium supplemented with 10 µg/mL BDNF and 10 µg/mL Rock Inhibitor Y-27632. The following day, media was changed to Synaptojuice medium 1 (N2B27 medium, 2 µM PD0332991 isethionate, 5 µM DAPT, 370 µM $CaCl_2$, 1 µM LM22A4, 2 µM CHIR99021, 300 µM GABA , and 10 µM NKH447) supplemented with 10 µg/mL BDNF. After 1 week, media was switched to Synaptojuice 2 (N2B27 medium, 2 µM PD0332991 isethionate, 370 µM $CaCl_2$, 1 µM LM22A4, and 2 µM CHIR99021) (Kemp et al. 2016). Cultures were maintained by media change every two days.

Preparation of drugs and chemicals

Peptides and small molecule drugs used in this study were reconstituted according to manufacturer instructions, aliquoted into single-use vials, and stored at -70°C or -20°C until the day of each experiment.

Calcium imaging

Calcium Imaging experiments were performed as previously described (Chen, Mazzaferro, et al. 2023). Briefly, hypothalamic progenitors differentiated from the HUES9-POMC-GFP cell line were replated onto 35 mm x 10 mm polystyrene imaging dishes (Corning) coated with 1 µg/cm^2 of iMatrix-511. All analyses were performed on neurons 40-50 days post-differentiation and transitioned from SynaptoJuice medium to BrainPhys medium 24-48 hours prior to recording. On the day of recording, neuronal cultures were loaded with Cal-590 AM fluorescent calcium indicator dye (Stratech) following manufacturers' instructions. An extracellular bath solution consisting of Hanks' Balanced Salt

Solution without Phenol Red (HBSS; ThermoFisher Scientific) and synaptic blockers were used for all aspects of calcium imaging, including dye loading, perfusion, and dilution of GLP1R agonists and other experimental substances. Synaptic blockers were added to final concentrations of 100 μM DL-AP5, 50 μM Picrotoxin, 30 μM CNQX, and 20 μM Strychnine to inhibit NDMA, GABA, AMPA/Kainate, and glycine receptors, respectively. Immediately before each experiment, GLP1R agonists were diluted from stock solutions to final concentrations of 200 nM in unless otherwise indicated.

Imaging dishes were placed on an Olympus BX51WI Fixed Stage Upright Microscope (RRID: SCR_023069) and imaged using a 16-bit high-speed ORCA Flash4.0 LT plus digital sCMOS camera (RRID: SCR_021971). Neurons were identified by Cal-590 AM fluorescence using an excitation wavelength of 540 nm and an emission wavelength of 590 nm. Images were taken using a 20x objective and acquired at a frequency of 0.1 Hz (100 ms exposure/frame) using a CoolLED pE-300 white illumination system (RRID: SCR_021073) and HCImage (RRID: SCR_015041) software for acquisition. Neurons were perfused continuously at room temperature (3 mL/min) using a gravity-driven perfusion system for the entire length of the experiment. For recordings, cells were perfused with extracellular bath solution for 10 minutes to record baseline fluorescence, and then perfused with extracellular bath solution containing the experimental compound for two minutes, followed by a second washout period (10-20 minutes) and stimulation with 50 mM KCl for two minutes followed by a washout period to identify responsive neurons. Videos of fluorescence intensity in the green (GFP) and red (Cal-590 AM) channels were recorded at an acquisition rate of 6 frames per minute.

Imaging and figure preparation

Images of hypothalamic cultures were collected on the calcium imaging microscope as described above, and separate cultures were plated onto PhenoPlateTM 96-well microplates (Perkin Elmer), fixed in 4% paraformaldehyde (Thermo Fisher Scientific) for 10 minutes, rinsed three times with Tris-buffered saline containing 0.1% Triton X-100 (TBS-T; Sigma-Aldrich), and incubated with primary antibodies including anti-αMSH (A1H5, detects epitopes in the αMSH region of POMC and developed by Professor Ann White; 1:5000) diluted in TBS-T containing 1% normal donkey serum (NDS; Stratech) overnight at 4 °C. Cells were washed three times with TBS-T and incubated with secondary antibodies diluted in TBS-T with 1% NDS for 2 hours at room temperature on an orbital shaker. Cells were washed three more times with TBS-T, and 300 μM of 4′,6-diamidino-2-phenylindole (DAPI; Thermo Fisher Scientific) was used to stain cell nuclei.

Image acquisition was performed using the Perkin Elmer Opera Phenix Plus High-Content Screening System with a 20x or 40x water objective. Some figure elements were prepared with the help of BioRender, and some photomicrographs were background-subtracted, adjusted for brightness and contrast, and false-colored to enable merging of channels and aid in visualization. Figures were prepared in Adobe Illustrator or Affinity Designer.

Quantification of responses from calcium imaging

To quantify changes in fluorescence intensity in GFP+ and GFP- neurons, regions of interest were manually drawn around candidate cells and raw fluorescence values from the 590 nm channel were exported to Microsoft Excel (RRID: SCR_016137) for each fluorescence time course. Only cells displaying a stable baseline prior to experimental compound administration and also a robust response to 50 mM KCl were considered for

analysis. The change in fluorescence intensity as a function of time was expressed as $(F - F_0)/F_0$ or $\Delta F/F_0$, where F was the measured fluorescence intensity and F_0 was the mean fluorescence intensity recorded during the 10 minute baseline period. Cellular responses to experimental compounds (e.g. GLP1R agonists) were quantified by comparing the change in the area under the curve (AUC) of normalized fluorescence ($\Delta F/F_0$) intensity in a three minute time window before and after addition of experimental compounds. The post-stimulus window started two minutes after compound administration to account for a slow rise in fluorescence intensity followed by a plateau period. We considered the raw $\Delta F/F_0$ values and did not normalize to KCl response amplitude.

Electrophysiology

Whole-cell recordings were obtained using the perforated Patch-Clamp technique as previously described (Goldspink et al. 2020). Briefly, microelectrodes were pulled from borosilicate glass (1.5 mm OD, 1.16 mm ID; Harvard Apparatus), and the tips were coated with refined yellow beeswax. Microelectrodes were fire-polished using a microforge (Narishige) and had resistances of 2-3 MΩ when filled with internal pipette solution. The internal pipette solution contained: 76 mM K_2SO_4, 10 mM NaCl, 10 mM KCl, 10 mM HEPES, 55 mM sucrose, and 1 mM $MgCl_2$; adjusted to pH 7.2 with KOH. Amphotericin B (10 µg/ml) dissolved in DMSO was added to the pipette solution on the day of recording to perforate cell membranes. A silver/AgCl wire connected to the bath solution via a 0.15 M NaCl agar bridge was used as a ground.

Once cells had been patched in this configuration (Lippiat 2008), recordings were acquired using an Axopatch 200B amplifier connected through a Digidata 1440A A/D converter and pCLAMP software (Molecular Devices). Spontaneous action potential firing was recorded in current-clamp mode without injecting current (I = 0). Neurons were perfused continuously at room temperature with HBSS solution (3 mL/min) in the presence of synaptic blockers using a gravity-driven perfusion system. For each experiment, we established a baseline recording period under perfusion, followed by perfusion with HBSS containing 200 nM Semaglutide. Membrane potential and the spontaneous action potential firing were recorded for 10-30 minutes before and after applying Semaglutide for six minutes. For each cell, mean membrane potential and action potential frequency was measured during 180 second-long time windows taken immediately before Semaglutide application, and 60-120 seconds after Semaglutide application, at which point Semaglutide induced depolarization had plateaued.

Semaglutide simulation and FACS purification of POMC neurons

To test for the transcriptional consequences of longer-term exposure to GLP1R agonists, HUES9-POMC-GFP hypothalamic cultures at 40 ± 2 days post-differentiation were cultured in N2B27 medium for 72 hours prior to treatment with vehicle (DMSO) or Semaglutide (2 µM, MedChem Express) in N2B27 medium for 20 hours. Cultures were then digested with TrypLE Express with 200 U/mL of papain and dissociated in wash media (N2B27) supplemented with 2 mg/mL DNAse I, 10 µg/mL Rock inhibitor, and 40 µg/mL actinomycin D. The cell suspension was centrifuged at 300 g for 5 min and washed with wash medium and centrifuged again. The resulting cell pellets were resuspended with 500 µL of sorting buffer ($DPBS^{-/-}$ with 1 mM EDTA, 25 mM HEPES, and 0.2% BSA) and transferred to DNA Lo-bind tubes for FACS sorting. Immediately prior to sorting, cells were filtered through a 40 µm Flowmi cell strainer and loaded onto the Aria Fusion Spyro set at 4°C and sorted using a 100 µm sort nozzle based on DAPI (0.1 µg/mL) for live/dead cells

and GFP fluorescence. Sorted live cells were collected directly into RLT lysis buffer and RNA was immediately extracted using the RNeasy Plus Micro kit (Qiagen).

Bulk RNA sequencing and analysis

RNA from sorted cells were analyzed on the Agilent 2100 Bioanalyser system using the Eukaryote Total RNA Pico kit (Agilent Technologies) and the mean RIN number was 9.5. Libraries of cDNA were then generated using the SMARTer Stranded Total RNA-Seq Kit v3 - Pico Input Mammalian (Takara). The resulting cDNA libraries were then quantified by the High Sensitivity DNA assay, pooled, and sequenced to a targeted depth of 50M reads/sample on Illumina flow cells to generate 100bp paired-end reads.

The resulting RNA sequencing libraries were pre-processed with TrimGalore (v0.6.7) (Krueger et al. 2021) to remove adapters and filter of low-quality reads before aligning them to the human (GRCh38, Ensembl release 98) reference genome using using STAR (v2.7.9a) (Dobin et al. 2013). Read counts per gene were then quantified using featureCounts (v2.0.0) (Liao, Smyth, and Shi 2014) against the human (GRCh38, gencode v32) annotation. Qualimap (v2.2.2d) (Okonechnikov, Conesa, and García-Alcalde 2015) was used to generate QC metrics of aligned reads for evaluating sample library quality, together with QC metrics produced by STAR and featureCounts. Size factor normalization and removal of lowly expressed genes was performed using edgeR. Further quality control analysis of the samples were performed using principal component analysis and expression correlation analysis to identify any outlier samples. For differential expression analysis, estimation of both negative binomial dispersions and quasi-likelihood dispersion were first performed using the edgeR package, followed by a quasi-likelihood F-test to identify genes which are differentially expressed between different treatment groups, with significance threshold set to FDR < 0.05. Finally, gene set enrichment analysis of the differentially expressed genes were performed using the g:Profiler R package (Raudvere et al. 2019), with custom background set to expressed gene list, analytical-adjusted p-value threshold set to 0.05 and data sources set to KEGG.

Statistical analysis

Graphing and statistical analysis were performed using GraphPad Prism (version 7.02; RRID: SCR_002798). For all one-way analyses of variance (ANOVA), data were first analyzed for normality using the D'agostino Pearson test. For all instances in which multiple paired t-tests were used, data were first analyzed for normality using the D'agostino Pearson test and results were presented as volcano plots with a P value < 0.01 adjusted by Holm-Sidak method. All the test data were executed with Welch's correction, which does not assume equal SD. For frequency analysis, data were organized in contingency tables and differences were tested by chi square test. Results were presented as mean with 95% CI for all calcium imaging experiments and mean ± standard error of the mean (SEM) for all other experiments. After adjusting for multiple comparisons, P values < 0.05 were considered as statistically significant.

Data, code, and materials availability

Upon publication in a peer-reviewed journal, sequencing data will be made available on ENA, and code used for analysis and generating figures will be made available in GitHub. Reagents will be made available upon request from the lead author (F.T.M.).

Acknowledgements

We thank Ann Cloos and Swetha Srinivasaraghavan for their assistance with hPSC culture and hypothalamic differentiation, Solomon Shepherd for providing images of live POMC-GFP cells, Anne White for providing anti-POMC antibodies, and Ben Jones from Imperial College London for helpful discussions. We are also grateful to Marcella Ma of the Genomics and Bioinformatics Core, which is funded by the UK Medical Research Council (MRC) Metabolic Disease Unit (MRC_MC_UU_00014/5) and a Wellcome Trust Major Award (208363/Z/17/Z), Chris Smith of the Tissue and Cell Imaging core facility for assistance with imaging, and the staff at the Genomics Core Facility of the Cancer Research UK Cambridge Institute for assistance with sequencing. F.T.M. is a New York Stem Cell Foundation - Robertson Investigator [NYSCF-R-156] and Chan Zuckerberg Initiative - Ben Barres Early Career Investigator [CZI NDCN 191942, 10.37921/429861umrcjh], and H-J.C.C., I.M., and A.Y. were supported by this funding. F.T.M. and S.M. and the costs of this study were supported by the Wellcome Trust and Royal Society [211221/Z/18/Z]. C.A. was supported by a Wellcome investigator award (220271/Z/20/Z), held by F.R. and F.M.G. D.S. is supported by the University of Cambridge within the Ukrainian Academic Support Scheme. For the purpose of open access, the authors have applied a CC-BY public copyright license to any Author Accepted Manuscript version arising from this submission.

Author contributions

The study was conceptualized by S.M. and F.T.M., who wrote the manuscript with the help of H.-J.C.C. and A.Y., and reviewing and editing contributions from all authors. F.T.M. acquired funding to support this work, administered the project, and supervised studies together with J.M. Data were collected and analyzed by S.M., O.C., A.Y., H.-J.C.C., C.A.A., and F.T.M., and visualized by S.M., H.-J.C.C., A.Y., and F.T.M. D.S., J.C., V.M., and I.M. helped generate cells and reagents, and provided intellectual contributions. J.M., F.G., and F.R. provided technical advice and intellectual contributions. Underlying methodologies were developed by S.M., H.-J.C.C., and O.C.

Declaration of interests

The authors declare no competing interests.

Inclusion and diversity

We support inclusive, diverse, and equitable conduct of research.

References

Acuna-Goycolea, Claudio, and Anthony van den Pol. 2004. “Glucagon-like Peptide 1 Excites Hypocretin/orexin Neurons by Direct and Indirect Mechanisms: Implications for Viscera-Mediated Arousal.” *The Journal of Neuroscience: The Official Journal of the Society for Neuroscience* 24 (37): 8141–52.

Aviles-Olmos, Iciar, John Dickson, Zinovia Kefalopoulou, Atbin Djamshidian, Peter Ell, Therese Soderlund, Peter Whitton, et al. 2013. “Exenatide and the Treatment of Patients with Parkinson’s Disease.” *The Journal of Clinical Investigation* 123 (6): 2730–36.

Aviles-Olmos, Iciar, John Dickson, Zinovia Kefalopoulou, Atbin Djamshidian, Joshua Kahan, Peter Ell, Peter Whitton, et al. 2014. “Motor and Cognitive Advantages Persist 12 Months after Exenatide Exposure in Parkinson’s Disease.” *Journal of Parkinson’s Disease* 4 (3): 337–44.

Baldini, Giulia, and Kevin D. Phelan. 2019. “The Melanocortin Pathway and Control of Appetite-Progress and Therapeutic Implications.” *The Journal of Endocrinology* 241 (1): R1–33.

Bessesen, Daniel H., and Luc F. Van Gaal. 2018. “Progress and Challenges in Anti-Obesity Pharmacotherapy.” *The Lancet. Diabetes & Endocrinology* 6 (3): 237–48.

Biebermann, Heike, Tamara R. Castañeda, Frank van Landeghem, Andreas von Deimling, Frederike Escher, Georg Brabant, Johannes Hebebrand, et al. 2006. “A Role for Beta-Melanocyte-Stimulating Hormone in Human Body-Weight Regulation.” *Cell Metabolism* 3 (2): 141–46.

Brennecke, Philip, Simon Anders, Jong Kyoung Kim, Aleksandra A. Kołodziejczyk, Xiuwei Zhang, Valentina Proserpio, Bianka Baying, et al. 2013. “Accounting for Technical Noise in Single-Cell RNA-Seq Experiments.” *Nature Methods* 10 (11): 1093–95.

Cachelin, A. B., J. E. de Peyer, S. Kokubun, and H. Reuter. 1983. “Ca2+ Channel Modulation by 8-Bromocyclic AMP in Cultured Heart Cells.” *Nature* 304 (5925): 462–64.

Chen, Hsiao-Jou Cortina, Simone Mazzaferro, Tian Tian, Iman Mali, and Florian T. Merkle. 2023. “Differentiation, Transcriptomic Profiling, and Calcium Imaging of Human Hypothalamic Neurons.” *Current Protocols* 3 (6): e786.

Chen, Hsiao-Jou Cortina, Andrian Yang, Simone Mazzaferro, Iman Mali, Olivier Cahn, Katherine Kentistou, Christine Rowley, et al. 2023. “Profiling Human Hypothalamic Neurons Reveals a Candidate Combination Drug Therapy for Weight Loss.” *bioRxiv*. https://doi.org/10.1101/2023.07.18.549357.

Cone, Roger D. 2005. “Anatomy and Regulation of the Central Melanocortin System.” *Nature Neuroscience* 8 (5): 571–78.

Coskun, Tamer, Kyle W. Sloop, Corina Loghin, Jorge Alsina-Fernandez, Shweta Urva, Krister B. Bokvist, Xuewei Cui, et al. 2018. “LY3298176, a Novel Dual GIP and GLP-1 Receptor Agonist for the Treatment of Type 2 Diabetes Mellitus: From Discovery to Clinical Proof of Concept.” *Molecular Metabolism* 18 (December): 3–14.

Coskun, Tamer, Shweta Urva, William C. Roell, Hongchang Qu, Corina Loghin, Julie S. Moyers, Libbey S. O’Farrell, et al. 2022. “LY3437943, a Novel Triple Glucagon, GIP, and GLP-1 Receptor Agonist for Glycemic Control and Weight Loss: From Discovery to Clinical Proof of Concept.” *Cell Metabolism* 34 (9): 1234–47.e9.

Cowley, M. A., J. L. Smart, M. Rubinstein, M. G. Cerdán, S. Diano, T. L. Horvath, R. D. Cone, and M. J. Low. 2001. “Leptin Activates Anorexigenic POMC Neurons through a Neural Network in the Arcuate Nucleus.” *Nature* 411 (6836): 480–84.

Dittmann, Marie T., Gabriella Lakatos, Jodie F. Wainwright, Jacek Mokrosinski, Eloise Cross, I. Sadaf Farooqi, Natalie J. Wallis, et al. 2024. “Low Resting Metabolic Rate and Increased Hunger due to β-MSH and β-Endorphin Deletion in a Canine Model.” *Science Advances* 10 (10): eadj3823.

Dolphin, Annette C. 2018. “Voltage-Gated Calcium Channels: Their Discovery, Function and Importance as Drug Targets.” *Brain and Neuroscience Advances* 2 (October). https://doi.org/10.1177/2398212818794805.

Dong, Yanbin, Jamie Carty, Nitsan Goldstein, Zhenyan He, Eunsang Hwang, Dominic Chau, Briana Wallace, et al. 2021. “Time and Metabolic State-Dependent Effects of GLP-1R Agonists on NPY/AgRP and POMC Neuronal Activity in Vivo.” *Molecular Metabolism* 54 (December): 101352.

During, Matthew J., Lei Cao, David S. Zuzga, Jeremy S. Francis, Helen L. Fitzsimons, Xiangyang Jiao, Ross J. Bland, et al. 2003. “Glucagon-like Peptide-1 Receptor Is Involved in Learning and Neuroprotection.” *Nature Medicine* 9 (9): 1173–79.

Egefjord, Lærke, Michael Gejl, Arne Møller, Hans Brændgaard, Hanne Gottrup, Olga Antropova, Niels Møller, et al. 2012. “Effects of Liraglutide on Neurodegeneration, Blood Flow and Cognition in Alzheimer´s Disease - Protocol for a Controlled, Randomized Double-Blinded Trial.” *Danish Medical Journal* 59 (10): A4519.

Farooqi, I. Sadaf, Julia M. Keogh, Giles S. H. Yeo, Emma J. Lank, Tim Cheetham, and Stephen O’Rahilly. 2003. “Clinical Spectrum of Obesity and Mutations in the Melanocortin 4 Receptor Gene.” *The New England Journal of Medicine* 348 (12): 1085–95.

Farooqi, Sadaf, and Stephen O’Rahilly. 2006. “Genetics of Obesity in Humans.” *Endocrine Reviews* 27 (7): 710–18.

Fenselau, Henning, John N. Campbell, Anne M. J. Verstegen, Joseph C. Madara, Jie Xu, Bhavik P. Shah, Jon M. Resch, et al. 2017. “A Rapidly Acting Glutamatergic ARC→PVH Satiety Circuit Postsynaptically Regulated by α-MSH.” *Nature Neuroscience* 20 (1): 42–51.

Gabery, Sanaz, Casper G. Salinas, Sarah J. Paulsen, Jonas Ahnfelt-Rønne, Tomas Alanentalo, Arian F. Baquero, Stephen T. Buckley, et al. 2020. “Semaglutide Lowers Body Weight in Rodents via Distributed Neural Pathways.” *JCI Insight* 5 (6). https://doi.org/10.1172/jci.insight.133429.

Gejl, M., A. Gjedde, L. Egefjord, A. Møller, S. B. Hansen, K. Vang, A. Rodell, et al. 2016. “In Alzheimer’s Disease, 6-Month Treatment with GLP-1 Analog Prevents Decline of Brain Glucose Metabolism: Randomized, Placebo-Controlled, Double-Blind Clinical Trial.” *Frontiers in Aging Neuroscience* 8 (May). https://doi.org/10.3389/fnagi.2016.00108.

Gejl, Michael, Birgitte Brock, Lærke Egefjord, Kim Vang, Jørgen Rungby, and Albert Gjedde. 2017. “Blood-Brain Glucose Transfer in Alzheimer’s Disease: Effect of GLP-1 Analog Treatment.” *Scientific Reports* 7 (1): 17490.

Glotfelty, Elliot J., Thomas Delgado, Luis B. Tovar-Y-Romo, Yu Luo, Barry Hoffer, Lars Olson, Tobias Karlsson, et al. 2019. “Incretin Mimetics as Rational Candidates for the Treatment of Traumatic Brain Injury.” *ACS Pharmacology & Translational Science* 2 (2): 66–91.

Goldspink, Deborah A., Van B. Lu, Emily L. Miedzybrodzka, Christopher A. Smith, Rachel E. Foreman, Lawrence J. Billing, Richard G. Kay, Frank Reimann, and Fiona M. Gribble. 2020. “Labeling and Characterization of Human GLP-1-Secreting L-Cells in Primary Ileal Organoid Culture.” *Cell Reports* 31 (13): 107833.

Gomez, Edith, Catrin Pritchard, and Terence P. Herbert. 2002. “cAMP-Dependent Protein Kinase and Ca2+ Influx through L-Type Voltage-Gated Calcium Channels Mediate Raf-Independent Activation of Extracellular Regulated Kinase in Response to Glucagon-like Peptide-1 in Pancreatic Beta-Cells.” *The Journal of Biological Chemistry* 277 (50): 48146–51.

Halawi, Houssam, Disha Khemani, Deborah Eckert, Jessica O’Neill, Hoda Kadouh, Karen Grothe, Matthew M. Clark, et al. 2017. “Effects of Liraglutide on Weight, Satiation, and Gastric Functions in Obesity: A Randomised, Placebo-Controlled Pilot Trial.” *The Lancet. Gastroenterology & Hepatology* 2 (12): 890–99.

Hayes, Matthew R., Theresa M. Leichner, Shiru Zhao, Grace S. Lee, Amy Chowansky, Derek Zimmer, Bart C. De Jonghe, Scott E. Kanoski, Harvey J. Grill, and Kendra K. Bence. 2011. “Intracellular Signals Mediating the Food Intake-Suppressive Effects of Hindbrain Glucagon-like Peptide-1 Receptor Activation.” *Cell Metabolism* 13 (3): 320–30.

He, Zhenyan, Yong Gao, Linh Lieu, Sadia Afrin, Jianhong Cao, Natalie J. Michael, Yanbin

Dong, Jia Sun, Hongbo Guo, and Kevin W. Williams. 2019. “Direct and Indirect Effects of Liraglutide on Hypothalamic POMC and NPY/AgRP Neurons - Implications for Energy Balance and Glucose Control.” *Molecular Metabolism* 28 (October): 120–34.

Hogg, Elliot, Tina Wu, Catherine Bresee, Jeffrey Wertheimer, Camille Malatt, Echo Tan, Hayley Pomeroy, Miriam Nuno, Richard Wyse, and Michele Tagliati. 2022. “A Phase II, Randomized, Double-Blinded, Placebo-Controlled Trial of Liraglutide in Parkinson’s Disease,” September. https://doi.org/10.2139/ssrn.4212371.

Huszar, D., C. A. Lynch, V. Fairchild-Huntress, J. H. Dunmore, Q. Fang, L. R. Berkemeier, W. Gu, et al. 1997. “Targeted Disruption of the Melanocortin-4 Receptor Results in Obesity in Mice.” *Cell* 88 (1): 131–41.

Irannejad, Roshanak, Jin C. Tomshine, Jon R. Tomshine, Michael Chevalier, Jacob P. Mahoney, Jan Steyaert, Søren G. F. Rasmussen, et al. 2013. “Conformational Biosensors Reveal GPCR Signalling from Endosomes.” *Nature* 495 (7442): 534–38.

Jastreboff, Ania M., Louis J. Aronne, Nadia N. Ahmad, Sean Wharton, Lisa Connery, Breno Alves, Arihiro Kiyosue, et al. 2022. “Tirzepatide Once Weekly for the Treatment of Obesity.” *The New England Journal of Medicine* 387 (3): 205–16.

Jones, Ben, Teresa Buenaventura, Nisha Kanda, Pauline Chabosseau, Bryn M. Owen, Rebecca Scott, Robert Goldin, et al. 2018. “Targeting GLP-1 Receptor Trafficking to Improve Agonist Efficacy.” *Nature Communications* 9 (1): 1602.

Jorgensen, Rasmus, Valentina Kubale, Milka Vrecl, Thue W. Schwartz, and Christian E. Elling. 2007. “Oxyntomodulin Differentially Affects Glucagon-like Peptide-1 Receptor Beta-Arrestin Recruitment and Signaling through Galpha(s).” *The Journal of Pharmacology and Experimental Therapeutics* 322 (1): 148–54.

Kanehisa, Minoru, Miho Furumichi, Yoko Sato, Masayuki Kawashima, and Mari Ishiguro-Watanabe. 2023. “KEGG for Taxonomy-Based Analysis of Pathways and Genomes.” *Nucleic Acids Research* 51 (D1): D587–92.

Kawatani, Masahiro, Yuichiro Yamada, and Masahito Kawatani. 2018. “Glucagon-like Peptide-1 (GLP-1) Action in the Mouse Area Postrema Neurons.” *Peptides* 107 (September): 68–74.

Kemp, Paul J., David J. Rushton, Polina L. Yarova, Christian Schnell, Charlene Geater, Jane M. Hancock, Annalena Wieland, et al. 2016. “Improving and Accelerating the Differentiation and Functional Maturation of Human Stem Cell-Derived Neurons: Role of Extracellular Calcium and GABA.” *The Journal of Physiology* 594 (22): 6583–94.

Kirwan, Peter, Magdalena Jura, and Florian T. Merkle. 2017. “Generation and Characterization of Functional Human Hypothalamic Neurons.” *Current Protocols in Neuroscience / Editorial Board, Jacqueline N. Crawley ... [et Al.]* 81 (October): 3.33.1–3.33.24.

Kirwan, Peter, Richard G. Kay, Bas Brouwers, Vicente Herranz-Pérez, Magdalena Jura, Pierre Larraufie, Julie Jerber, et al. 2018. “Quantitative Mass Spectrometry for Human Melanocortin Peptides in Vitro and in Vivo Suggests Prominent Roles for β-MSH and Desacetyl α-MSH in Energy Homeostasis.” *Molecular Metabolism* 17 (November): 82–97.

Klaauw, Agatha A. van der, Sophie Croizier, Edson Mendes de Oliveira, Lukas K. J. Stadler, Soyoung Park, Youxin Kong, Matthew C. Banton, et al. 2019. “Human Semaphorin 3 Variants Link Melanocortin Circuit Development and Energy Balance.” *Cell* 176 (4): 729–42.e18.

Knerr, Patrick J., Stephanie A. Mowery, Jonathan D. Douros, Bhavesh Premdjee, Karina Rahr Hjøllund, Yantao He, Ann Maria Kruse Hansen, et al. 2022. “Next Generation GLP-1/GIP/glucagon Triple Agonists Normalize Body Weight in Obese Mice.” *Molecular Metabolism* 63 (September): 101533.

Kopp, Katherine O., Elliot J. Glotfelty, Yazhou Li, and Nigel H. Greig. 2022. “Glucagon-like Peptide-1 (GLP-1) Receptor Agonists and Neuroinflammation: Implications for Neurodegenerative Disease Treatment.” *Pharmacological Research: The Official Journal of the Italian Pharmacological Society* 186 (December): 106550.

Krude, H., H. Biebermann, W. Luck, R. Horn, G. Brabant, and A. Grüters. 1998. “Severe

Early-Onset Obesity, Adrenal Insufficiency and Red Hair Pigmentation Caused by POMC Mutations in Humans." *Nature Genetics* 19 (2): 155–57.
Lau, Jesper, Paw Bloch, Lauge Schäffer, Ingrid Pettersson, Jane Spetzler, Jacob Kofoed, Kjeld Madsen, et al. 2015. "Discovery of the Once-Weekly Glucagon-Like Peptide-1 (GLP-1) Analogue Semaglutide." *Journal of Medicinal Chemistry* 58 (18): 7370–80.
Lee, Yung Seng, Ben G. Challis, Darren A. Thompson, Giles S. H. Yeo, Julia M. Keogh, Michael E. Madonna, Vicki Wraight, et al. 2006. "A POMC Variant Implicates Beta-Melanocyte-Stimulating Hormone in the Control of Human Energy Balance." *Cell Metabolism* 3 (2): 135–40.
Lippiat, Jonathan D. 2008. "Whole-Cell Recording Using the Perforated Patch Clamp Technique." *Methods in Molecular Biology* 491: 141–49.
Li, Yazhou, Tracyann Perry, Mark S. Kindy, Brandon K. Harvey, David Tweedie, Harold W. Holloway, Kathleen Powers, et al. 2009. "GLP-1 Receptor Stimulation Preserves Primary Cortical and Dopaminergic Neurons in Cellular and Rodent Models of Stroke and Parkinsonism." *Proceedings of the National Academy of Sciences of the United States of America* 106 (4): 1285–90.
Locke, Adam E., Bratati Kahali, Sonja I. Berndt, Anne E. Justice, Tune H. Pers, Felix R. Day, Corey Powell, et al. 2015. "Genetic Studies of Body Mass Index Yield New Insights for Obesity Biology." *Nature* 518 (7538): 197–206.
Loos, Ruth J. F., and Giles S. H. Yeo. 2022. "The Genetics of Obesity: From Discovery to Biology." *Nature Reviews. Genetics* 23 (2): 120–33.
Meier, Juris J. 2012. "GLP-1 Receptor Agonists for Individualized Treatment of Type 2 Diabetes Mellitus." *Nature Reviews. Endocrinology* 8 (12): 728–42.
Merkle, Florian T., Asif Maroof, Takafumi Wataya, Yoshiki Sasai, Lorenz Studer, Kevin Eggan, and Alexander F. Schier. 2015. "Generation of Neuropeptidergic Hypothalamic Neurons from Human Pluripotent Stem Cells." *Development* 142 (4): 633–43.
Mitchell, James L., Hannah S. Lyons, Jessica K. Walker, Andreas Yiangou, Olivia Grech, Zerin Alimajstorovic, Nigel H. Greig, et al. 2023. "The Effect of GLP-1RA Exenatide on Idiopathic Intracranial Hypertension: A Randomized Clinical Trial." *Brain: A Journal of Neurology* 146 (5): 1821–30.
Mitterdorfer, J., M. Froschmayr, M. Grabner, F. F. Moebius, H. Glossmann, and J. Striessnig. 1996. "Identification of PK-A Phosphorylation Sites in the Carboxyl Terminus of L-Type Calcium Channel Alpha 1 Subunits." *Biochemistry* 35 (29): 9400–9406.
Müller, T. D., B. Finan, S. R. Bloom, D. D'Alessio, D. J. Drucker, P. R. Flatt, A. Fritsche, et al. 2019. "Glucagon-like Peptide 1 (GLP-1)." *Molecular Metabolism* 30 (December): 72–130.
NCD Risk Factor Collaboration (NCD-RisC). 2024. "Worldwide Trends in Underweight and Obesity from 1990 to 2022: A Pooled Analysis of 3663 Population-Representative Studies with 222 Million Children, Adolescents, and Adults." *The Lancet* 403 (10431): 1027–50.
Panagaki, Theodora, Simon Gengler, and Christian Hölscher. 2018. "The Novel DA-CH3 Dual Incretin Restores Endoplasmic Reticulum Stress and Autophagy Impairments to Attenuate Alzheimer-Like Pathology and Cognitive Decrements in the APPSWE/PS1ΔE9 Mouse Model." *Journal of Alzheimer's Disease: JAD* 66 (1): 195–218.
Péterfi, Zoltán, Anett Szilvásy-Szabó, Erzsébet Farkas, Yvette Ruska, Charles Pyke, Lotte Bjerre Knudsen, and Csaba Fekete. 2021. "Glucagon-Like Peptide-1 Regulates the Proopiomelanocortin Neurons of the Arcuate Nucleus Both Directly and Indirectly via Presynaptic Action." *Neuroendocrinology* 111 (10): 986–97.
Qiu, J., E. J. Wagner, O. K. Rønnekleiv, and M. J. Kelly. 2018. "Insulin and Leptin Excite Anorexigenic pro-Opiomelanocortin Neurones via Activation of TRPC5 Channels." *Journal of Neuroendocrinology* 30 (2). https://doi.org/10.1111/jne.12501.
Quarta, Carmelo, Marc Claret, Lori M. Zeltser, Kevin W. Williams, Giles S. H. Yeo, Matthias H. Tschöp, Sabrina Diano, Jens C. Brüning, and Daniela Cota. 2021. "POMC Neuronal Heterogeneity in Energy Balance and beyond: An Integrated View." *Nature Metabolism*

3 (3): 299–308.
Raudvere, Uku, Liis Kolberg, Ivan Kuzmin, Tambet Arak, Priit Adler, Hedi Peterson, and Jaak Vilo. 2019. “g:Profiler: A Web Server for Functional Enrichment Analysis and Conversions of Gene Lists (2019 Update).” *Nucleic Acids Research* 47 (W1): W191–98.
Reich, Niklas, and Christian Hölscher. 2022. “The Neuroprotective Effects of Glucagon-like Peptide 1 in Alzheimer’s and Parkinson's Disease: An in-Depth Review.” *Frontiers in Neuroscience* 16 (September): 970925.
Rønnekleiv, Oline K., Yuan Fang, Chunguang Zhang, Casey C. Nestor, Peizhong Mao, and Martin J. Kelly. 2014. “Research Resource: Gene Profiling of G Protein-Coupled Receptors in the Arcuate Nucleus of the Female.” *Molecular Endocrinology* 28 (8): 1362–80.
Secher, Anna, Jacob Jelsing, Arian F. Baquero, Jacob Hecksher-Sørensen, Michael A. Cowley, Louise S. Dalbøge, Gitte Hansen, et al. 2014. “The Arcuate Nucleus Mediates GLP-1 Receptor Agonist Liraglutide-Dependent Weight Loss.” *The Journal of Clinical Investigation* 124 (10): 4473–88.
Shilleh, Ali H., Katrina Viloria, Johannes Broichhagen, Jonathan E. Campbell, and David J. Hodson. 2024. “GLP1R and GIPR Expression and Signaling in Pancreatic Alpha Cells, Beta Cells and Delta Cells.” *Peptides* 175 (February): 171179.
Singh, Ishnoor, Le Wang, Baijuan Xia, Ji Liu, Azeddine Tahiri, Abdelfattah El Ouaamari, Michael B. Wheeler, and Zhiping P. Pang. 2022. “Activation of Arcuate Nucleus Glucagon-like Peptide-1 Receptor-Expressing Neurons Suppresses Food Intake.” *Cell & Bioscience* 12 (1): 178.
Sonoda, Noriyuki, Takeshi Imamura, Takeshi Yoshizaki, Jennie L. Babendure, Juu-Chin Lu, and Jerrold M. Olefsky. 2008. “Beta-Arrestin-1 Mediates Glucagon-like Peptide-1 Signaling to Insulin Secretion in Cultured Pancreatic Beta Cells.” *Proceedings of the National Academy of Sciences of the United States of America* 105 (18): 6614–19.
Steuernagel, Lukas, Brian Y. H. Lam, Paul Klemm, Georgina K. C. Dowsett, Corinna A. Bauder, John A. Tadross, Tamara Sotelo Hitschfeld, et al. 2022. “HypoMap-a Unified Single-Cell Gene Expression Atlas of the Murine Hypothalamus.” *Nature Metabolism* 4 (10): 1402–19.
Tadross, John A., Lukas Steuernagel, Georgina K. C. Dowsett, Katherine A. Kentistou, Sofia Lundh, Marta Porniece-Kumar, Paul Klemm, et al. 2023. “Human HYPOMAP: A Comprehensive Spatio-Cellular Map of the Human Hypothalamus.” *bioRxiv*. https://doi.org/10.1101/2023.09.15.557967.
Tan, Qiming, Seun E. Akindehin, Camila E. Orsso, Richelle C. Waldner, Richard D. DiMarchi, Timo D. Müller, and Andrea M. Haqq. 2022. “Recent Advances in Incretin-Based Pharmacotherapies for the Treatment of Obesity and Diabetes.” *Frontiers in Endocrinology* 13 (March): 838410.
Vadini, Francesco, Paola G. Simeone, Andrea Boccatonda, Maria T. Guagnano, Rossella Liani, Romina Tripaldi, Augusto Di Castelnuovo, Francesco Cipollone, Agostino Consoli, and Francesca Santilli. 2020. “Liraglutide Improves Memory in Obese Patients with Prediabetes or Early Type 2 Diabetes: A Randomized, Controlled Study.” *International Journal of Obesity* 44 (6): 1254–63.
Wilding, John P. H., Rachel L. Batterham, Salvatore Calanna, Melanie Davies, Luc F. Van Gaal, Ildiko Lingvay, Barbara M. McGowan, et al. 2021. “Once-Weekly Semaglutide in Adults with Overweight or Obesity.” *The New England Journal of Medicine* 384 (11): 989–1002.
Wootten, Denise, Christopher A. Reynolds, Kevin J. Smith, Juan C. Mobarec, Cassandra Koole, Emilia E. Savage, Kavita Pabreja, et al. 2016. “The Extracellular Surface of the GLP-1 Receptor Is a Molecular Trigger for Biased Agonism.” *Cell* 165 (7): 1632–43.
Wu, Peipei, Yuxiao Zhao, Xianghua Zhuang, Aili Sun, Yuan Zhang, and Yihong Ni. 2018. “Low Glucagon-like Peptide-1 (GLP-1) Concentration in Serum Is Indicative of Mild Cognitive Impairment in Type 2 Diabetes Patients.” *Clinical Neurology and Neurosurgery* 174 (November): 203–6.
Yaswen, L., N. Diehl, M. B. Brennan, and U. Hochgeschwender. 1999. “Obesity in the Mouse

Model of pro-Opiomelanocortin Deficiency Responds to Peripheral Melanocortin." *Nature Medicine* 5 (9): 1066–70.
Yeo, Giles S. H., Emma J. Lank, I. Sadaf Farooqi, Julia Keogh, Benjamin G. Challis, and Stephen O'Rahilly. 2003. "Mutations in the Human Melanocortin-4 Receptor Gene Associated with Severe Familial Obesity Disrupts Receptor Function through Multiple Molecular Mechanisms." *Human Molecular Genetics* 12 (5): 561–74.
Zamponi, Gerald W., Joerg Striessnig, Alexandra Koschak, and Annette C. Dolphin. 2015. "The Physiology, Pathology, and Pharmacology of Voltage-Gated Calcium Channels and Their Future Therapeutic Potential." *Pharmacological Reviews* 67 (4): 821–70.
Zhao, Fenghui, Qingtong Zhou, Zhaotong Cong, Kaini Hang, Xinyu Zou, Chao Zhang, Yan Chen, et al. 2022. "Structural Insights into Multiplexed Pharmacological Actions of Tirzepatide and Peptide 20 at the GIP, GLP-1 or Glucagon Receptors." *Nature Communications* 13 (1): 1–16.

Figures and Figure Legends

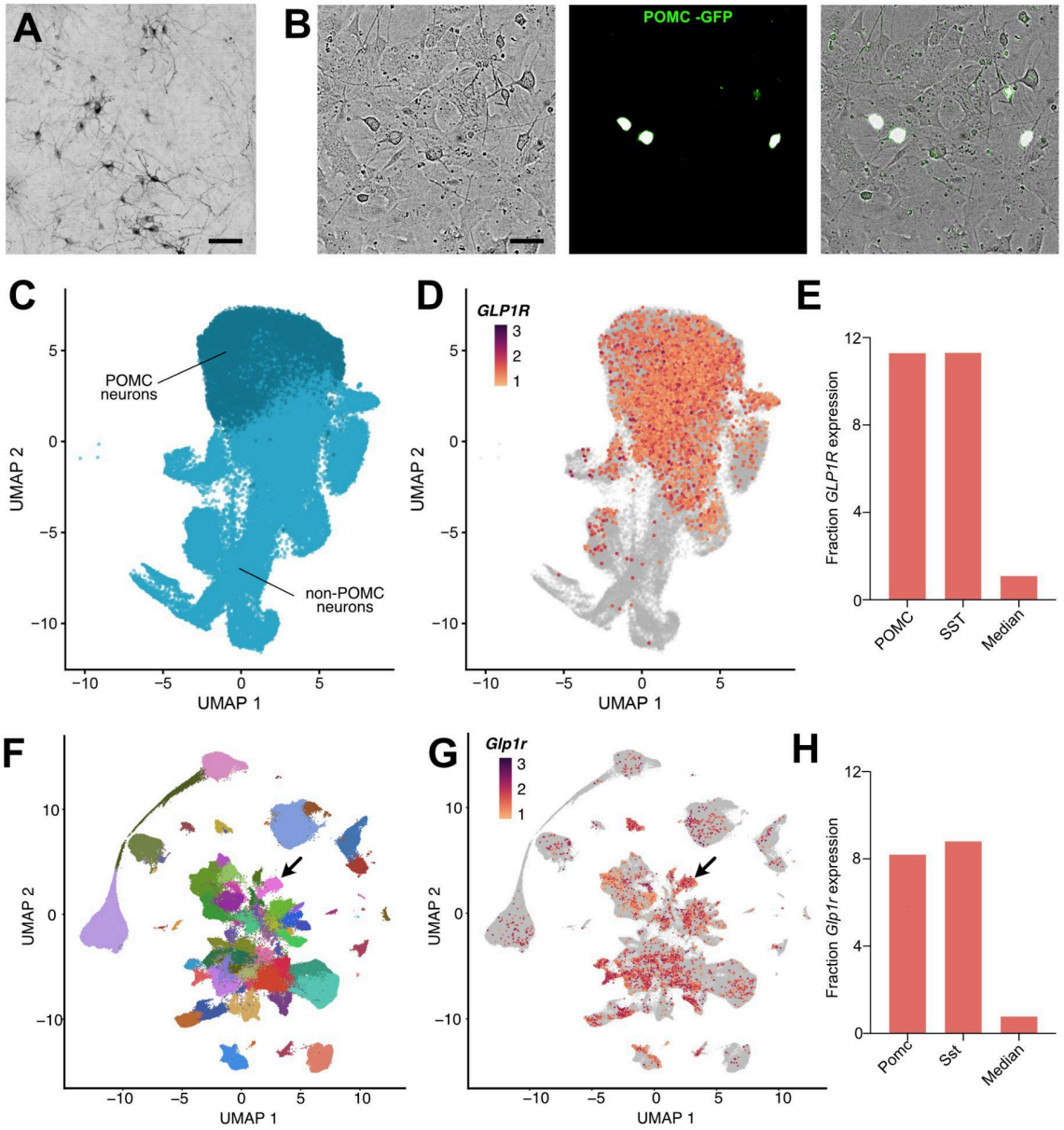

Figure 1. Expression of GLP1R mRNA in human POMC neurons. A,B) Hypothalamic cells differentiated from human pluripotent stem cells (hPSCs) contain a significant number of POMC neurons as visualized by immunostaining for aMSH (A) and in live cultures derived from a POMC-GFP reporter cell line (B). Scale bars represent 25 and 12 µm in A and B, respectively. **C)** UMAP of single-cell RNAseq data from five genetically distinct hPSC lines differentiated into hypothalamic neurons, separated by cells annotated as being in POMC (dark blue) or non-POMC (light blue) clusters. **D,E)** Expression of *GLP1R* mRNA in hPSC-derived hypothalamic neurons (UMI ≥ 1), color-coded by expression level (D) and quantified for POMC or SST cell clusters, and median expression across all cell clusters (E). **F)** UMAP with 66 annotated clusters from mouse single-cell and single-nucleus RNAseq data, with the arrowhead indicating the Pomc-expressing cell cluster. **G,H)** Expression of *Glp1r* mRNA in mouse hypothalamic neurons (UMI ≥ 1), color-coded by expression level (G) or quantified across Pomc or Sst clusters, or the median across all cell clusters.

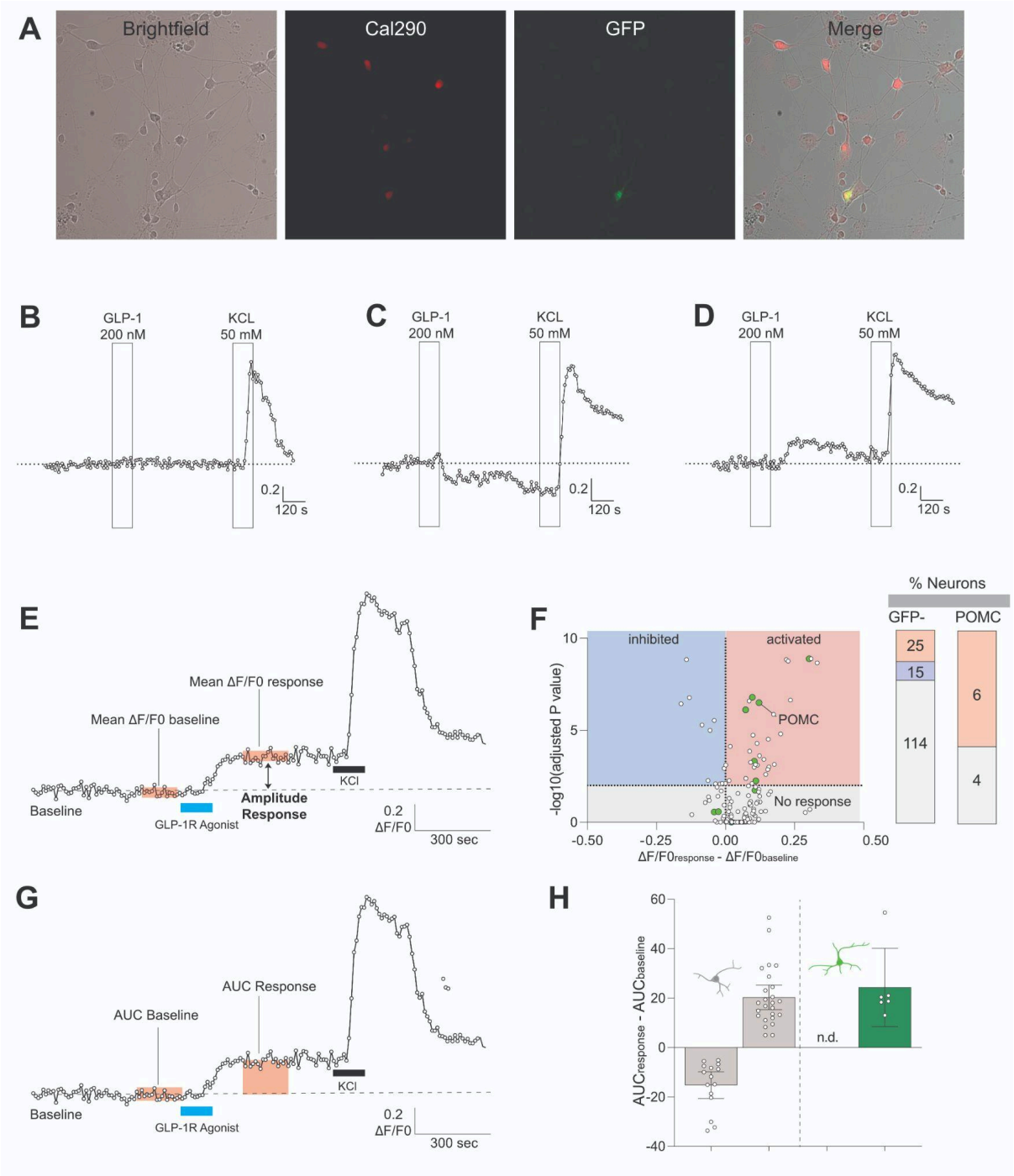

Figure 2. Responses of human hypothalamic neurons to GLP1. A) Photomicrographs from a POMC-GFP reporter cell line showing (from left to right) neuronal morphology in brightfield, baseline fluorescence from the Cal-590 AM calcium sensitive dye, endogenous GFP fluorescence from the reporter, and a merge of these images. **B-D)** Representative traces from single neurons in response to administration of 200 nM GLP-1 for two minutes showing no response (B), decreased fluorescence (C), a prolonged increase in fluorescence (D), where the Y axis represents $\Delta F/F_0$. **E)** Representative trace showing how GLP1R responsive cells were classified by calculating whether values for $\Delta F/F_0$ taken in a baseline period were significantly different from those taken after GLP1R agonist administration. **F)** Plot of the significance of response probability (Y axis) versus the magnitude of response ($\Delta F/F_0$), where GFP+ POMC neurons are plotted in green, and a cutoff of $P<0.01$ was used to assign cells into inhibited (blue), activated (red), and non-responsive (gray) categories. Significance was calculated by multiple paired t-test from 18 pre-stimulus and 18 post-stimulus fluorescence intensity values. **G)** Representative trace showing how the magnitude of response to GLP1R was calculated by taking the area under the curve (AUC) in three-minute time intervals before and after its administration. **H)** Summary of the activated and inhibited cell responses for GFP- and POMC neurons. Non-responsive neurons are not shown.

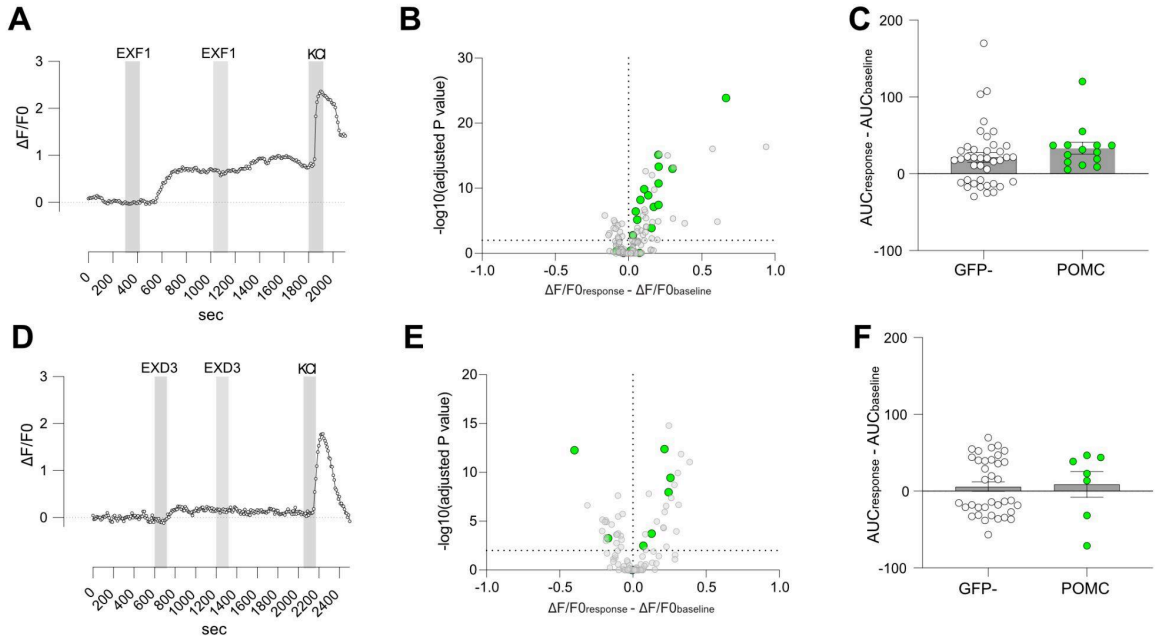

Figure 3. Neuronal responses to GLP1R 'biased' agonists. A) Representative calcium imaging trace of a cell responding to a two-minute administration of Ex-F1, and then responding to a second administration given 10 minutes later. **B)** Distribution of the significance and magnitude of response to Ex-F1 across all analyzed cells. **C)** Response magnitude to Ex-F1 in activated and inhibited GFP- and POMC neurons. **D-F)** As in A-C above but for Ex-D3, for which calcium responses to a second administration after a 10 minute delay were not observed. Significance calculated by Welch's t test .

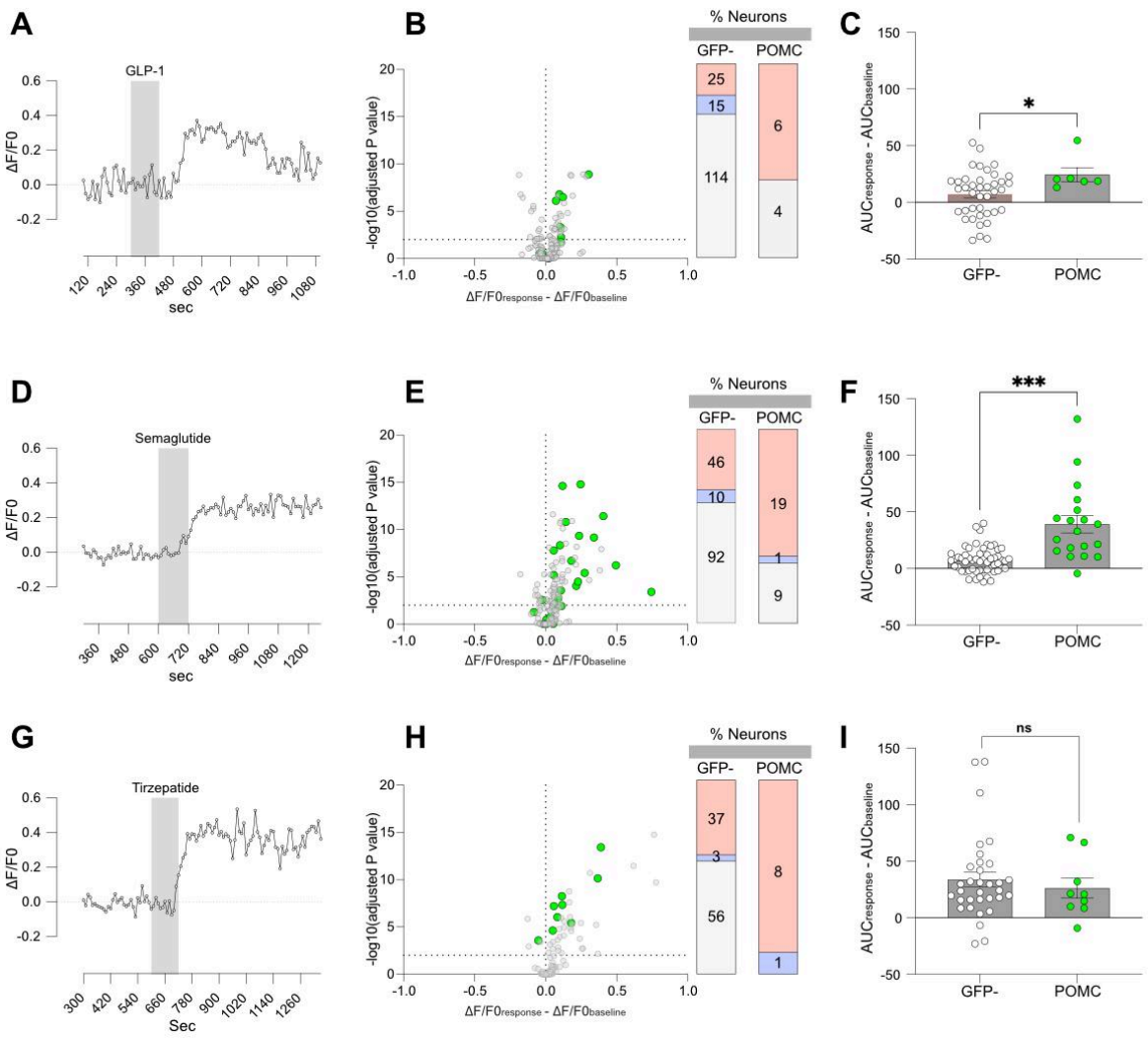

Figure 4. Effects of anti-obesity drugs on human hypothalamic neurons. A-C) Representative calcium imaging trace of a cell responding to 200 nM GLP-1 peptide (A), the classification of neuronal responses into activated, inhibited and non-responsive as described in Figure 2, and the fraction of GFP- and POMC neurons in each of these categories (B), comparison of responses between GFP- and POMC neurons (C). **D-I)** Panels as in A-C, but for 200 nM Semaglutide (D-F), or 200 nM Tirzepatide (G-I). Significance calculated by chi-squared test in B, E, H, and Welch's t test in C, F, I, where *p<0.05, **p<0.001.

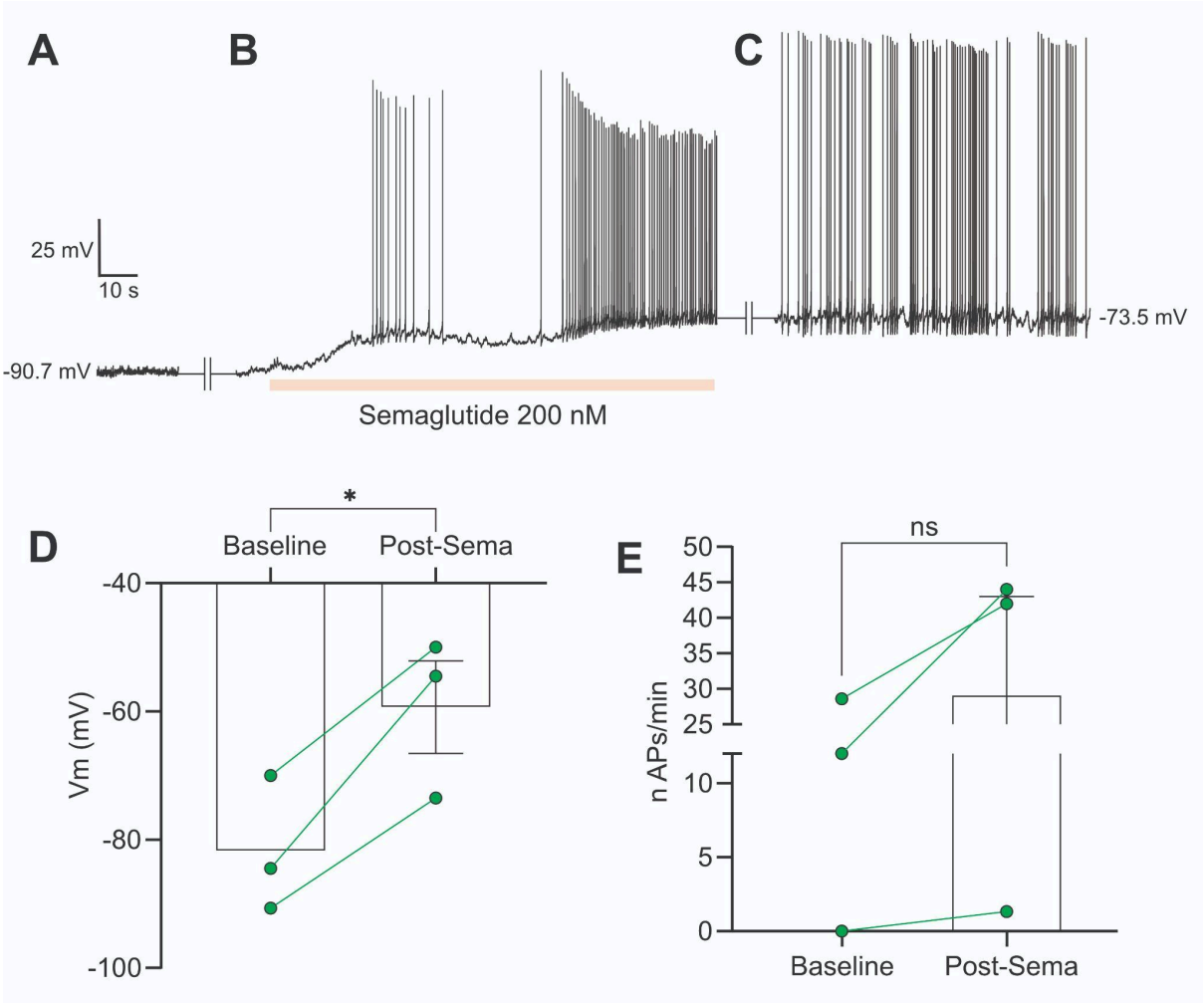

Figure 5. Electrophysiological analysis of POMC neuron responses to Semaglutide. A-C) Representative trace of a hPSC-derived POMC neuron under perforated patch preparation that is relatively quiescent under baseline conditions (A, see also E) but is depolarized upon administration of 200 nM Semaglutide leading to an increased rate action potential firing (B) that persists for up to at least 20 minutes after Semaglutide withdrawal (C). **D)** POMC neuron Vm shifts to a significantly ($P<0.05$) depolarised state after addition of 200 nM Semaglutide (Post-Sema). N=3 cells. Significance calculated by paired t test. **E)** All tested POMC neurons show an increase in average action potential (AP) firing rate per minute in response to 200 nM Semaglutide (Post-Sema).

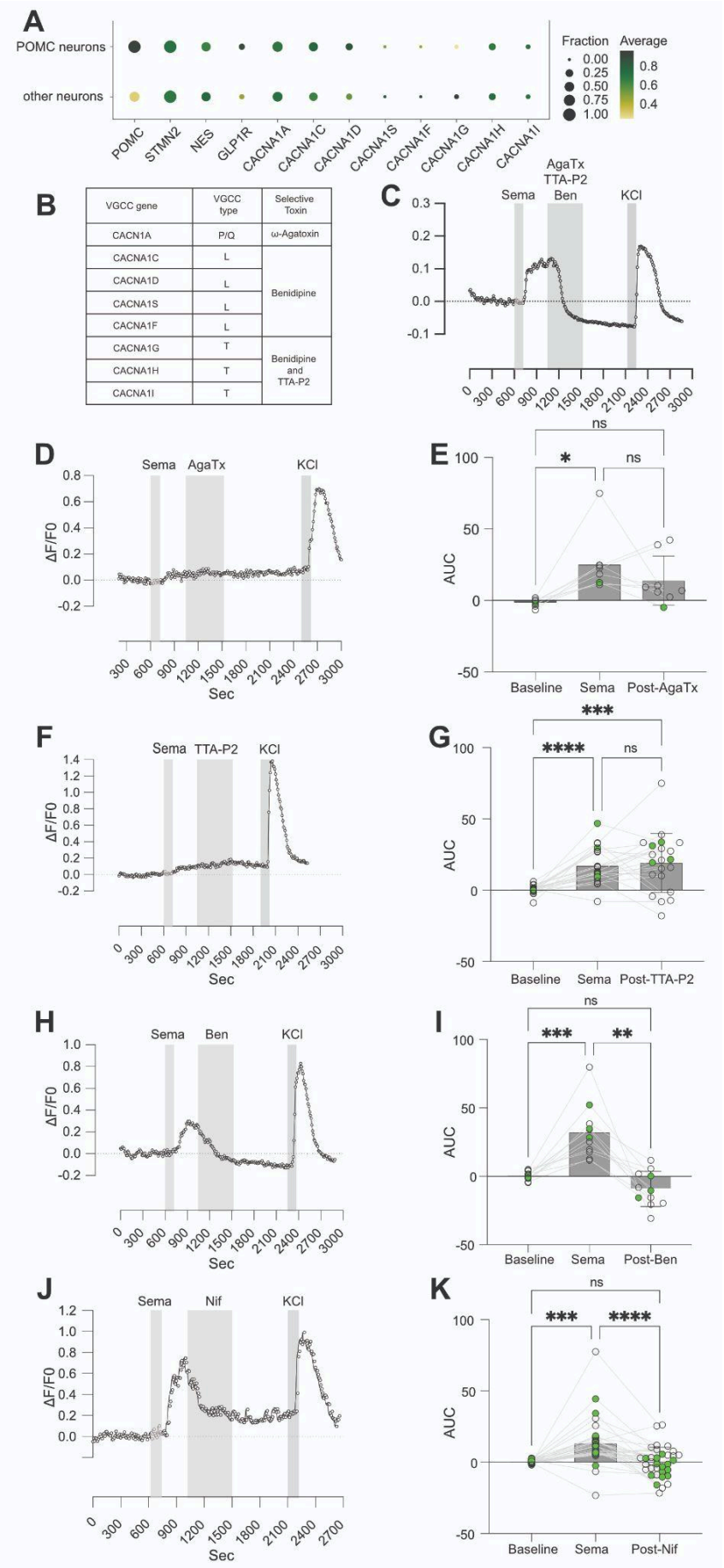

VGCC gene	VGCC type	Selective Toxin
CACN1A	P/Q	ω-Agatoxin
CACNA1C	L	Benidipine
CACNA1D	L	
CACNA1S	L	
CACNA1F	L	
CACNA1G	T	Benidipine and TTA-P2
CACNA1H	T	
CACNA1I	T	

Figure 6. GLP1R agonist-induced calcium responses require voltage-gated calcium channels. A) Normalized expression levels (low to high = yellow to dark green) of candidate genes from scRNAseq data of hPSC-derived hypothalamic POMC neurons (top row), or non-POMC neurons (bottom row), where dot size indicates the fraction of cells in each population in which the candidate gene was detected (UMI ≥ 1). *POMC*, *GLP1R*, and *CACNA1D* are significantly enriched in POMC neurons. **B)** Table of voltage-gated calcium channel (VGCC) gene names, channel type, and the identity of drugs that selectively inhibit them. **C)** In a Semaglutide-activated cell, a cocktail of VGCC blockers abolishes agonist-induced fluorescence of the calcium indicator. **D,E)** Administration of the P/Q-type VGCC blocker ω-Agatoxin does not significantly decrease Semaglutide-induced calcium indicator fluorescence, as seen in a representative trace (D) and in a summary of all Semaglutide-activated cells (E). **F,G)** Panels as in D,E but with the T-type VGCC blocker TTA-P2. **H,I)** Panels as in D-G, but with the L-type VGCC blocker Benidipine, which abolished Semaglutide-induced calcium dye fluorescence, as observed with the drug cocktail in (C). **J,K)** Panels as in D-I, showing that the results from Benidipine (H,I) are replicated with Nifedipine, a second L-type calcium channel blocker. *$p<0.05$, **$p<0.01$, ***$p<0.001$ ****$p<0.0001$ by one-way ANOVA with repeated measures in E, G, I, K.

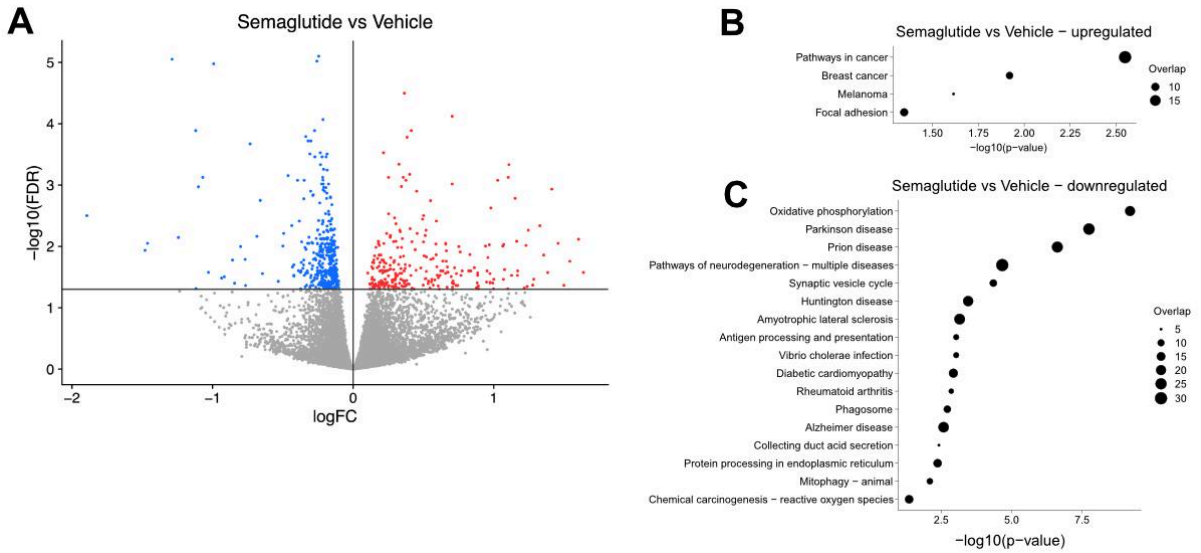

Figure 7. Transcriptional effects of GLP1R activation in POMC neurons. A) Volcano plot of significantly differentially expressed genes between vehicle- and Semaglutide-treated POMC neurons, with a cutoff of FDR<0.05, **B,C)** KEGG enrichment of analysis of significantly (FDR <0.05) upregulated (C), or downregulated (D) genes.